

Evolution and fluctuations of chiral chemical potential in heavy ion collisions

Vladimir Kovalenko *

*Saint Petersburg State University,
7/9 Universitetskaya Nab., St. Petersburg 199034, Russia
v.kovalenko@spbu.ru*

The possible appearance of the effects of local parity breaking in the QCD medium formed in heavy ion collisions due to violation of chiral symmetry can be quantified by corresponding chiral chemical potential μ_5 . The experimental observables sensitive to the effects of local parity violation in strong interaction include search for polarisation splitting of the ρ_0 and ω_0 mesons via angular dependence of spectral functions in their decay to leptons. In this paper we study the space-time evolution and fluctuations of μ_5 using relativistic hydrodynamics and estimate their effect on the light vector meson polarization splitting in Pb-Pb collisions at LHC energy.

Keywords: local parity violation; chiral imbalance; chiral chemical potential; relativistic hydrodynamics

PACS numbers: 11.30.Er, 11.30.Rd, 24.10.Nz, 13.20.-v

1. Introduction

The strong interaction, as it is well known, obey the global spatial (P) parity conservation. So far, no evidence has been found for violation of P- and CP-symmetries in strong interactions. However, quantum chromodynamics (QCD) does not forbid the local parity symmetry breaking due to large topological fluctuations at high temperature with dynamic generation of nontrivial topological charge configurations. A necessary condition for observing these effects is a sufficiently large space dimension and a long lifetime of a hot drop of QCD medium, which is available in central nuclear-nuclear collisions at the LHC [1–3].

In the presence of a hot medium in the state of deconfinement, formed in heavy ion collisions, the modification of the properties of hadrons is possible. They can arise due to the inhomogeneity of the medium, as well as due to such non-perturbative effects as, for example, instantons [4]. In the perturbative calculations, the amplitudes of transitions between different degenerate vacua, connected by topologically non-trivial gauge transformations, are equal to zero in any order of the perturbation theory. However, they can afford for nonperturbative phenomena, known as sphaleron transition [5–7], happening through a potential barrier sepa-

*Corresponding author.

rating topologically nonequivalent vacua. Such configurations can be excited in the collision of heavy ions, or initially exist in them [1, 2].

So it can be assumed that parity-violating bubbles can arise in a collision of relativistic nuclei in a finite volume, causing the effect of a local parity nonconservation. The behavior of the topological charge of the gauge fields existing in a fireball for a long time, in statistical approach, can be described in terms of topological chemical potential (μ_θ). Due to the partial nonconservation of the axial current in QCD, in the approximation of low fermion masses, it is possible to relate the topological charge to the value of the chiral imbalance, which is defined as the average difference between the number of right and left quarks in a fireball after heavy ion collisions at high energy [8]. Thus, chiral imbalance can lead to the formation of local parity violation (LPB) in a quark-hadron medium with local thermodynamic equilibrium characterized by an axial chemical potential [9]. In this case, a connection arises between the topological (μ_θ) and axial (μ_5) chemical potentials:

$$\mu_5 = \frac{1}{N_f} \mu_\theta, \quad (1)$$

where N_f is a number of flavors.

The effect of local parity nonconservation in strong interactions can be experimentally searched for using local observables sensitive to the processes at hadron space scale, which are not canceled out after the summation over the whole medium.

It was shown in [10–13] that this effect can be verified experimentally by analyzing the yields of dilepton pairs in the region of small invariant masses in heavy ion collisions. This will require simultaneous scanning of both the invariant mass (m_{ll}) and the expansion angle (θ_A) of leptons from the decays of light vector mesons. In the case of a nonzero axial chemical potential, a polarization splitting of the spectral functions of ρ and ω mesons occurs in a part of the phase space, with the formation of a characteristic two-peak structure.

Later, it was shown [14] that if the radiative corrections are taken into account, then the presence of the axial chemical potential leads not only to the splitting of the masses of the left and right polarizations of vector mesons, but also to their general shift towards an increase. These effects depend both on the value of the axial chemical potential μ_5 and on the momentum of the vector meson (k).

Because the polarization mass splitting depends on the axial chemical potential μ_5 , the experimentally measured picture would depend also on the fluctuations of μ_5 . There is a risk that in case of sufficiently large fluctuations the splitting would smear out and become hard to detect. So the main purpose of the paper is to investigate the evolution of the axial charge density during heavy ion collision from the initial stages to freeze-out and to estimate its fluctuations induced by this evolution.

We should add that other ways of observation of parity nonconservation effects in heavy ion collisions are possible. In the presence of the large magnetic field,

which is characterized by semi-central and peripheral ion collisions, the so-called chiral magnetic effect (CME) can happen [9,15]. It was measured at RHIC and LHC [16–18] and a CME-like signal was found. However, other backgrounds, like a local charge conservation, play a comparable role [19]. Nevertheless, the comparison of the experimental results with modelling [20] showed the best agreement is achieved for the μ_5 above 300 MeV.

The other possibilities, suitable also for central heavy ion collisions, include the search for decays of a scalar charged a_0 meson into a photon and a charged pion or into three charged pions [21–24]; study the relative rate of pi-meson decay by muon-neutrino and electron-neutrino channels [24]; search for possible asymmetry of the photon polarization [25].

2. Methods

The simulation of the evolution of the QCD medium produced in heavy ion collisions at LHC energy has been performed using relativistic hydrodynamics. A commonly-used package MUSIC [26–29], 3+1D relativistic second-order viscous hydrodynamics for heavy ion collisions, was used. In this studies, for simplicity, boost-invariant 2+1D version was taken. Lattice hotQCD equation of state (EOS) was used, and no dependence in EOS on μ_5 were assumed.

The initial energy density distributions were generated using Glauber Monte Carlo sampler [30,31] with energy density deposited at wounded nucleon positions. Central Pb-Pb collisions at 5.02 TeV (with impact parameter $b \leq 2$ fm) were considered.

The initial axial charge densities were set up as negative and positive isolated areas in the transverse plane with radius of 2.1 fm with the constant ρ_5 inside them and zero total axial charge (see Figure 1).

The freezeout condition was set as the minimal energy density of $\text{Ed}=0.18 \text{ GeV/fm}^3$. Because the effect of the vector meson polarization splitting equally depends on the positive and negative axial charge, at the freezeout the distribution of the absolute value of the axial charge density is obtained.

To calculate the di-lepton invariant masses spectra, a Monte Carlo model based on the Pythia 8 event generator was used (version 8.2) [32] with built-in Angantyr collision model for relativistic nuclei [33]. For the simulations, collisions of lead nuclei at an energy of 5.02 TeV were used. In order to increase the statistics of the di-lepton spectrum, the fraction of decays of ρ and ω mesons through the di-electron and di-muon channels was increased up to 0.44.

Decay products were considered in the following rapidity intervals:

$$-0.8 < \eta < 0.8 \text{ for electrons, } -3.6 < \eta < -2.45 \text{ for muons.}$$

This corresponds to the range of the time projection camera and the internal tracking system of the ALICE experiment at the LHC in the central rapidity region and the muon system in the forward rapidity region [34]. At was initially proposed,

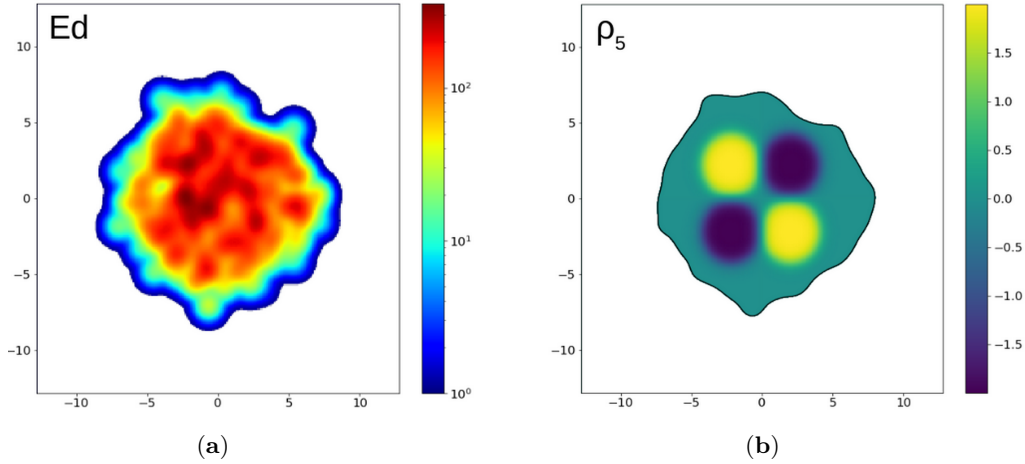


Fig. 1. The initial distribution of energy density (a) and axial charge density (b) in the transverse plane as an example for one Pb-Pb collision event at an energy of 5.02 TeV.

to perform the angular analysis in the central rapidity region [13] and ensure the equal treatment of both the di-muon and di-electron channels, for all muon tracks we applied a boost along the z axis by rapidity of 3.05 so that in the new reference frame they lie in the midrapidity. Only di-leptons coming from the decay of light vector mesons were kept for analysis, and background events were not taken into account.

The spectral functions of ρ and ω mesons are shifted in presence of the non-zero chiral charge so that their masses depend on the μ_5 and momentum k as [14]:

$$m_{\rho,\omega}^* = m_{\rho,\omega} + 0.23 \mu_5^2 + 1.37 \mu_5 k + 2.54 \mu_5^2 k^2 \quad (2)$$

(here $m_{\rho,\omega}^*$, $m_{\rho,\omega}$, μ_5 , k are in GeV).

Then the leptons momentum is smeared in order to take into account the experimental resolution. The parameters were taken as for the ALICE experiment in the LHC Run 3 conditions (after the LS2 upgrade) [35–37]. The resulting standard deviation of transverse momentum for electrons was taken as 1% and for muons as 0.5%.

Then the di-lepton distributions are calculated with some cuts on the angle θ_A between the leptons [13]. The cuts are selected to keep the reasonable statistics but ensure as good as possible the separate the lepton polarisations.

3. Results

The initial distributions of energy density and axial charge density over the transverse plane are shown in Figure 1 for one example Pb-Pb event.

Then the medium undergo the hydrodynamic evolution. Some intermediate stages are shown in Figure 2. On the 2nd and 3rd panels the snapshots of the axial charge density at the fixed energy density are plotted, which approximately correspond to the fixed proper time τ . The results demonstrate that some smearing is happening and also the neutral area in the center is increasing, however overall the local charge excess stays throughout the entire evolution up to the freezeout. Due to expansion, the overall scale of the charge density decreases.

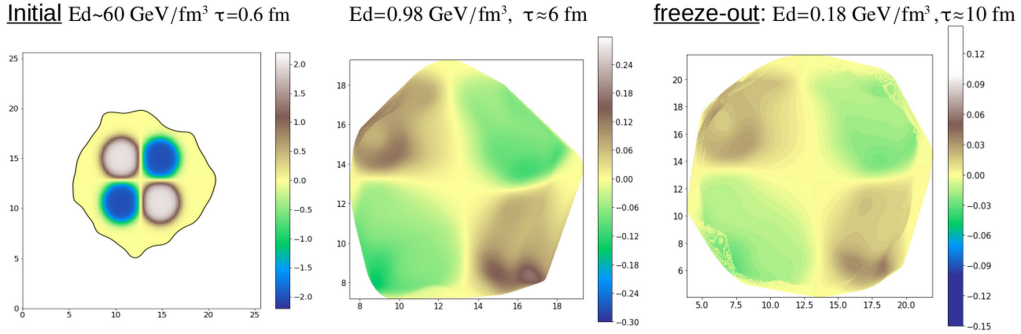


Fig. 2. Hydrodynamic evolution of the axial charge density from initial states to freezeout, an example for one Pb-Pb collision event at an energy of 5.02 TeV.

Because the effects depend on the absolute value of the axial charge, in Figure 3 we show the distribution of the absolute value of the axial density at the moment of freezeout and calculate the mean value $|\rho_5|$ and standard deviation $\sigma_{|\rho_5|}$ of this distribution.

Then the value of relative fluctuation $\delta_{|\rho_5|} = \sigma_{|\rho_5|} / \langle |\rho_5| \rangle$ is calculated. After the event-by-event study of this value the following result was obtained: $\delta_{|\rho_5|} = 0.42 \pm 0.04$.

Taking into account the estimation of the axial charge density fluctuation we can include it in the calculation of the di-lepton mass distributions. In case of the local thermodynamic equilibrium the axial charge density and axial chemical potential are related, and in the range of our consideration (a few hundreds MeV) the dependence is close to linear. So we put $\delta_{|\rho_5|} \approx \delta_{|\mu_5|}$.

In the Figure 4 the di-electron and di-muon mass distributions are plotted taken into account the fluctuation of the axial chemical potential at the level of 40%, the experimental resolution of ALICE in the Run 3 conditions and the kinematic cuts and selection with angle θ_A between leptons (also shown in the figure). The mean value of axial chemical potential was taken as $\mu_5 = 0.15$ GeV. The results show that the separation of at least two polarisations both for electrons and muons is visible in this conditions.

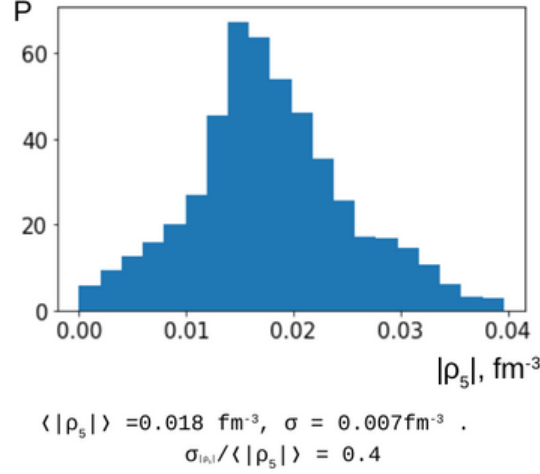


Fig. 3. Distribution of the absolute value of the axial charge density at the freezeout.

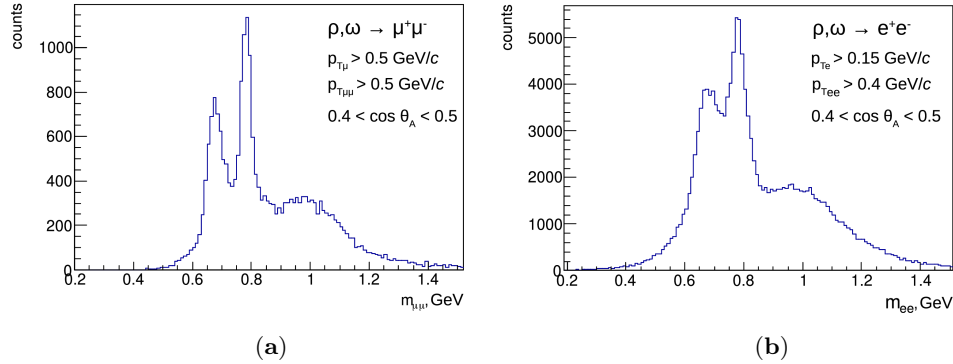


Fig. 4. Invariant mass distribution of di-muons **(a)** and di-electrons **(b)** in the Monte Carlo model from the decays of ρ and ω mesons under the expected conditions of the ALICE Run 3 experiment at μ_5 distributed according to Gauss with a mean of 0.15 GeV and a standard deviation $\sigma_{\mu_5} = 0.06$ GeV ($\delta_{\mu} = 40\%$).

4. Discussion

The evolution of the axial chemical potential during hydrodynamical expansion of the QCD medium, produced in Pb-Pb collisions at LHC energy, has been studied. The results show that the regions of local axial charge excess survive in the medium throughout the entire evolution of the fireball from the initial stages to freezeout. The resulting smearing induced by the hydrodynamical evolution is obtained at the level of 40%.

Study of the influence of such fluctuation on the possibility of detecting the local space parity nonconservation via angular analysis of di-lepton distribution showed

that such fluctuations do not destroy the possibility of observing the splitting of vector meson polarizations in the conditions the LHC Run 3 data.

We should note that our work cover only hydrodynamical evolution of the axial charge, and the possible instanton effects are not taken into account. We also has not considered any border effects and treated the borders smoothly. Also the initial conditions for the ρ_5 distributions are taken quite arbitrary. These points can be addressed in the further development of the work.

Acknowledgements

The study was funded by the Russian Science Foundation grant No. 22-22-00493, <https://rscf.ru/en/project/22-22-00493/>

ORCID

Vladimir Kovalenko  <https://orcid.org/0000-0001-6012-6615>

References

1. D. Kharzeev and A. Zhitnitsky. Charge separation induced by P-odd bubbles in QCD matter. *Nucl. Phys. A*, 797:67–79, 2007.
2. K. Buckley, T. Fugleberg, and A. Zhitnitsky. Can theta vacua be created in heavy ion collisions? *Phys. Rev. Lett.*, 84:4814–4817, 2000.
3. D. T. Son and Ariel R. Zhitnitsky. Quantum anomalies in dense matter. *Phys. Rev. D*, 70:074018, 2004.
4. A.A. Belavin, A.M. Polyakov, A.S. Schwartz, and Yu.S. Tyupkin. Pseudoparticle solutions of the yang-mills equations. *Physics Letters B*, 59(1):85–87, 1975.
5. Larry McLerran, Emil Mottola, and Mikhail E. Shaposhnikov. Sphalerons and axion dynamics in high-temperature qcd. *Phys. Rev. D*, 43:2027–2035, 1991.
6. Guy D. Moore and Kari Rummukainen. Classical sphaleron rate on fine lattices. *Phys. Rev. D*, 61:105008, 2000.
7. Edward Shuryak and Ismail Zahed. Prompt quark production by exploding sphalerons. *Phys. Rev. D*, 67:014006, 2003.
8. Dmitri Kharzeev, Robert D. Pisarski, and Michel H. G. Tytgat. Possibility of spontaneous parity violation in hot qcd. *Phys. Rev. Lett.*, 81:512–515, 1998.
9. Dmitri Kharzeev. Parity violation in hot QCD: Why it can happen, and how to look for it. *Phys. Lett. B*, 633:260–264, 2006.
10. A.A. Andrianov, V.A. Andrianov, D. Espriu, and X. Planells. Dilepton excess from local parity breaking in baryon matter. *Physics Letters B*, 710(1):230–235, 2012.
11. Alexander Andrianov, Vladimir A. Andrianov, Domenec Espriu, and Xumeu Planells. Abnormal dilepton yield from parity breaking in dense nuclear matter. *AIP Conf. Proc.*, 1343:450–452, 2011.
12. Xumeu Planells Noguera, Alexander Andrianov, Vladimir Andrianov, and Domenec Espriu. QCD effective theories with external chemical potentials. *PoS, QFTHEP* 2013:049, 2014.
13. A. A. Andrianov, V. A. Andrianov, D. Espriu, and X. Planells. Analysis of dilepton angular distributions in a parity breaking medium. *Phys. Rev. D*, 90:034024, 2014.
14. V Kovalenko, A Andrianov, and V Andrianov. Vector mesons spectrum in a medium

- with a chiral imbalance induced by the vacuum of fermions. *Journal of Physics: Conference Series*, 1690(1):012097, 2020.
15. Dmitri E. Kharzeev, Larry D. McLerran, and Harmen J. Warringa. The effects of topological charge change in heavy ion collisions: “event by event p and cp violation”. *Nuclear Physics A*, 803(3):227–253, 2008.
 16. Gang Wang. Experimental overview of the search for chiral effects at rhic. *Journal of Physics: Conference Series*, 779(1):012013, 2017.
 17. Md. Rihan Haque. Measurements of the chiral magnetic effect in pb–pb collisions with alice. *Nuclear Physics A*, 982:543–546, 2019. The 27th International Conference on Ultrarelativistic Nucleus-Nucleus Collisions: Quark Matter 2018.
 18. Sizar Aziz. Search for the Chiral Magnetic Effect with the ALICE detector. *Nucl. Phys. A*, 1005:121817, 2021.
 19. Xu-Guang Huang. Electromagnetic fields and anomalous transports in heavy-ion collisions—a pedagogical review. *Reports on Progress in Physics*, 79(7):076302, 2016.
 20. Zilin Yuan, Anping Huang, Wen-Hao Zhou, Guo-Liang Ma, and Mei Huang. Evolution of topological charge through chiral anomaly transport. 10 2023.
 21. Alexander Andrianov, Vladimir Andrianov, and Domenec Espriu. QCD with Chiral Imbalance: models vs. lattice. *EPJ Web Conf.*, 137:01005, 2017.
 22. A. A. Andrianov, V. A. Andrianov, D. Espriu, A. E. Putilova, and A. V. Iakubovich. Decays of light mesons triggered by chiral chemical potential. *Acta Phys. Polon. Supp.*, 10:977, 2017.
 23. A. A. Andrianov, V. A. Andrianov, D. Espriu, A. V. Iakubovich, and A. E. Putilova. QCD with Chiral Chemical Vector: Models Versus Lattices. *Phys. Part. Nucl. Lett.*, 15(4):357–361, 2018.
 24. Alexander Andrianov, Vladimir Andrianov, and Domenec Espriu. Chiral perturbation theory vs. linear sigma model in a chiral imbalance medium. *Particles*, 3(1):15–22, Jan 2020.
 25. Putilova, A.E., Iakubovich, A.V., Andrianov, A.A., Andrianov, V.A., and Espriu, D. Exotic meson decays and polarization asymmetry in hadron environment with chiral imbalance. *EPJ Web Conf.*, 191:05014, 2018.
 26. Bjoern Schenke, Sangyong Jeon, and Charles Gale. (3+1)D hydrodynamic simulation of relativistic heavy-ion collisions. *Phys. Rev. C*, 82:014903, 2010.
 27. Bjorn Schenke, Sangyong Jeon, and Charles Gale. Higher flow harmonics from (3+1)D event-by-event viscous hydrodynamics. *Phys. Rev. C*, 85:024901, 2012.
 28. Jean-François Paquet, Chun Shen, Gabriel S. Denicol, Matthew Luzum, Björn Schenke, Sangyong Jeon, and Charles Gale. Production of photons in relativistic heavy-ion collisions. *Phys. Rev. C*, 93(4):044906, 2016.
 29. Jean-François Paquet. Simulating heavy ion collisions with MUSIC, Available online: https://webhome.phy.duke.edu/~jp401/music_manual/ (accessed on 29.01.2023) .
 30. Chun Shen. superMC, Monte Carlo event generator of initial density distributions for relativistic heavy-ion collisions, Available online: <https://github.com/chunshen1987/superMC> (accessed on 29.01.2023) .
 31. Chun Shen, Zhi Qiu, Huichao Song, Jonah Bernhard, Steffen Bass, and Ulrich Heinz. The iEBE-VISHNU code package for relativistic heavy-ion collisions. *Comput. Phys. Commun.*, 199:61–85, 2016.
 32. Torbjörn Sjöstrand, Stefan Ask, Jesper R. Christiansen, Richard Corke, Nishita Desai, Philip Ilten, Stephen Mrenna, Stefan Prestel, Christine O. Rasmussen, and Peter Z. Skands. An introduction to PYTHIA 8.2. *Comput. Phys. Commun.*, 191:159–177, 2015.
 33. Christian Bierlich, Gösta Gustafson, Leif Lönnblad, and Harsh Shah. The Angantyr

- model for Heavy-Ion Collisions in PYTHIA8. *JHEP*, 10:134, 2018.
34. Aamodt K. et al (ALICE Collaboration). The alice experiment at the cern lhc. *Journal of Instrumentation*, 3(08):S08002, 2008.
 35. Abelev B. et al (ALICE Collaboration). Technical design report for the upgrade of the alice inner tracking system. *Journal of Physics G: Nuclear and Particle Physics*, 41(8):087002, 2014.
 36. Edmundo Garcia-Solis. Perspectives of the ALICE Experiment and Detector Upgrade. *Nucl. Part. Phys. Proc.*, 267-269:382–391, 2015.
 37. Adam J. et al (ALICE Collaboration). Technical Design Report for the Muon Forward Tracker. Technical report, CERN-LHCC-2015-001, ALICE-TDR-018, 2015, <https://cds.cern.ch/record/1981898>.